

UDC 621.644

https://doi.org/10.33619/2414-2948/103/33

WAYS TO PROTECT EQUIPMENT FROM HYDRAULIC SHOCK

©*Fang Yilin*, ORCID: 0009-0008-6217-0749, Ogarev Mordovia State University,
Saransk, Russia, hey_ffylin@163.com

©*Kudashev S.*, SPIN-code: 4763-0003, Ph.D., Ogarev Mordovia State University,
Saransk, Russia, kudashev@mail.ru

СПОСОБЫ ЗАЩИТЫ ОБОРУДОВАНИЯ ОТ ГИДРАВЛИЧЕСКОГО УДАРА

©*Фан Илья*, ORCID: 0009-0008-6217-0749, Национальный исследовательский Мордовский
государственный университет им. Н.П. Огарева, г. Саранск, Россия, hey_ffylin@163.com

©*Кудашев С. Ф.*, SPIN-код: 4763-0003, канд. техн. наук, Национальный исследовательский
Мордовский государственный университет им. Н. П. Огарева,
г. Саранск, Россия, kudashev@mail.ru

Abstract. The hydraulic equipment is experiencing damage to its components and even the mechanical equipment owing to hydraulic shock induced by a sudden rise in load, resulting in a step reaction in the hydraulic system. An analysis of the hydraulic system is conducted to protect the equipment from the detrimental effects of hydraulic shock. This analysis includes examining components such as the hydraulic damper, centrifugal pump, accumulator, control valve, and others. The primary function of the power component is to mitigate hydraulic stress by altering the pump's flow rate. The control element initiates the reversing of the valve in the hydraulic system in order to mitigate hydraulic shock. The auxiliary components primarily concentrate on enhancing the efficiency of the accumulator and maximizing the synergistic utilization of damping components. By adjusting the input value, one may regulate the flow rate and pressure of the system. The discussion revolves around finding the most efficient frequency in the shortest amount of time.

Аннотация. Гидравлическое оборудование испытывает повреждения своих компонентов и даже механического оборудования из-за гидравлического удара, вызванного внезапным увеличением нагрузки, что приводит к ступенчатой реакции в гидравлической системе. Проводился анализ гидравлической системы для защиты оборудования от вредного воздействия гидравлического удара. Этот анализ включает изучение таких компонентов, как гидравлический демпфер, центробежный насос, аккумулятор, регулирующий клапан и другие. Основная функция компонента питания заключается в уменьшении гидравлического напряжения путем изменения расхода насоса. Элемент управления инициирует обратную сторону клапана в гидравлической системе для смягчения гидравлического удара. Вспомогательные компоненты в первую очередь направлены на повышение эффективности аккумулятора и максимизацию синергетического использования демпинговых компонентов. Регулируя входное значение, можно регулировать расход и давление системы. Дискуссия вращается вокруг поиска наиболее эффективной частоты в кратчайшие сроки.

Keywords: hydraulic shock, hydraulic system, properties research, energy chain calculation.

Ключевые слова: гидравлический удар, гидравлическая система, исследования свойств, расчет энергетической цепи.

Within the hydraulic system, frequent occurrences of high-pressure and variable-load working situations can lead to a lack of smoothness in the operation. Hence, it is imperative to configure the damping element settings of the system to not only fulfill the requirements of system throttle, pressure regulation, and other functions, but also to accomplish the objectives of system speed and pressure control [1]. Additionally, it is crucial to achieve the buffer and vibration damping function in order to address system movement issues, enhance system reliability, and ensure optimal handling. Hydraulic shock is the term used to describe a sudden increase in hydraulic pressure within a hydraulic circuit [2]. This spike in pressure leads to high peaks and is typically accompanied by vibration and noise. As a result, certain hydraulic components may malfunction, leading to equipment damage. The occurrence of hydraulic shock in the operation of different machinery is a common and inherent phenomenon. It is triggered by mechanical vibrations, ruptures in hydraulic lines, and the water hammer effect. The hydraulic shock phenomenon occurs due to a multitude of factors, encompassing a range of issues. Recently, scholars have suggested many methods to prevent hydraulic shock, mostly by focusing on the components of the hydraulic system [3].

The hydraulic system comprises hydraulic dampers, centrifugal pumps, accumulators, control valves, and several other components. A hydraulic damper is a mechanism designed to mitigate the effects of vibration and shock by absorbing them and regulating the velocity and displacement of the linked equipment. Additionally, it serves as a safeguarding mechanism that counterbalances displacements resulting from thermal expansion and contraction of the equipment [5]. It is crucial for maintaining system stability. Simultaneously, hydraulic dampers and damping holes regulate the flow to decelerate alterations and minimize oscillation.

Centrifugal pumps are fluid devices that operate based on the principle of centrifugal force. The primary body of the centrifugal pump is composed of two main components: the impeller and the worm shell. Compared to other types of fluid machinery, the structure of the centrifugal pump is comparatively uncomplicated [4]. The primary areas of research in the field of pumps are focused on enhancing stability, prolonging service life, and reducing energy usage. Prior to activation, it is necessary to ensure that the pump casing and suction pipe are completely filled with water. Once this is done, the motor can be started, causing the pump shaft to drive the impeller and initiate a rapid rotating motion of the water. The water undergoes centrifugal movement as it is propelled towards the outer edge of the impeller. This occurs through the vortex-shaped pump casing and flow channel, ultimately entering the pressurized water pipeline of the pump.

Hydraulic accumulators play three primary functions within the broader hydraulic system. There are three major purposes for a hydraulic accumulator: as an auxiliary power source, to compensate for leaks and maintain system pressure, and to absorb the impact pressure or pulsing pressure of the hydraulic pump [6]. The hydraulic impactor's impact piston is specifically designed for reciprocating motion inside the workflow. The piston only does external work during the stroke, while the return stage is only dedicated to preparing for the next stroke. During the return movement, the hydraulic pump is unable to provide enough hydraulic oil to meet the required amount for the piston's stroke. As a result, the entire system temporarily stores the excess oil in the accumulator. This is done to reduce the resistance during the return process. When the piston returns, the oil is discharged back into the tank of the accumulator. This not only improves the system's efficiency but also allows the accumulator to absorb any hydraulic shocks caused by sudden stops or reversals of the hydraulic cylinder, sudden closures or reversals of the reversing valve, or sudden stops of the hydraulic pump. This helps prevent damage to the system's components by avoiding excessively high system pressure.

The control valve facilitates the transmission and regulation of power in the hydraulic system by means of throttling and overflow [7]. However, this process results in significant energy loss inside the hydraulic system, manifesting as throttling loss and overflow loss, ultimately being converted into heat energy in the form of oil. The purpose of this part is to elucidate the hydraulic and heat transport phenomena by employing differential equations. To describe the process, begin by constructing an energy circuit and formulating the equation [0]. Then, input and output the energy through a black box and calculate the equation using the black box [0]. Next, write the image equation and derive the equation for complex resistance. Identify the coefficient and establish the frequency function of the energy circuit. Differentiate the real and imaginary parts of the complex resistance. Finally, based on this information, compute the amplitude-frequency characteristics and phase-frequency characteristics. The graph and conclusion are derived from the computed findings of amplitude-frequency characteristics and phase-frequency characteristics. Figure 1 depicts the experimental setup for hydraulic dampening of the pump. The hot water or steam generated in the boiler 1 reaches the hydraulic accumulator 4 through the shock valve 2, the centrifugal pump 3 and the check valve 5. When the shock valve 2 is closed, the reverse wave of the water hammer will go along the chain: a centrifugal pump; a check valve; a hydraulic accumulator; the pipeline. At the same time, the pressure in the accumulator increases, and kinetic energy is converted into potential. The principle of operation of the installation is shown in Figure 2. The heat transfer principle is shown in Figure 5. Figure 2 displays the location where the hydraulic energy chain will be constructed.

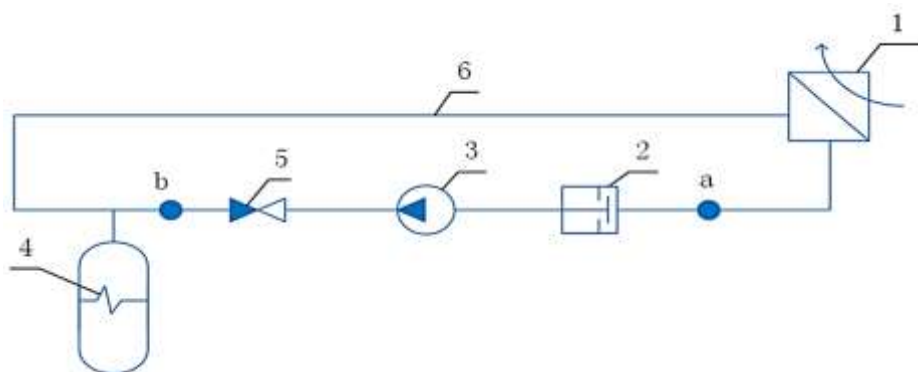


Figure 1. Experimental device for hydraulic dampening of pump. 1-boiler; 2-shock valve; 3-centrifugal pump; 4-hydraulic accumulator; 5-check valve; 6-pipeline

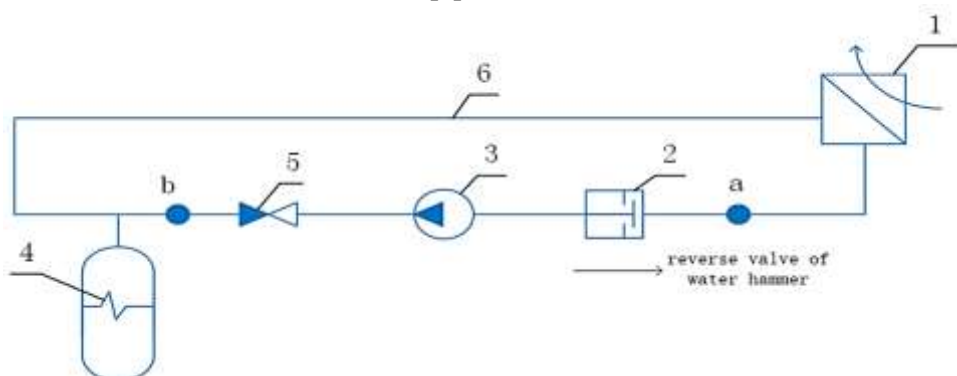


Figure 2. Plot for calculating the hydraulic energy circuit. 1-boiler; 2-shock valve; 3-centrifugal pump; 4-hydraulic accumulator; 5-check valve; 6-pipeline.

After filling the circuit with coolant, the centrifugal pump 3 turns on. When the set flow rate (over 1 m/s) is reached, the shock valve 2 closes. With the rapid closure of the impact valve 2, the

kinetic energy of the flow turns into potential energy, accompanied by an increase in pressure in front of the impact valve 2 (point a). Next, the wave of increased pressure will go in the opposite direction from point a to point b. Passing through the boiler 1, it will increase heat transfer, and before point b, it will be partially extinguished in the accumulator 4. As shown in Figure 3, in the course of the study, for a better understanding of the scheme, it was decided to study 2 characteristics of hydraulic and thermal, in order to better understand the nature of the forces arising and to more accurately determine the required parameters on the obtained model.

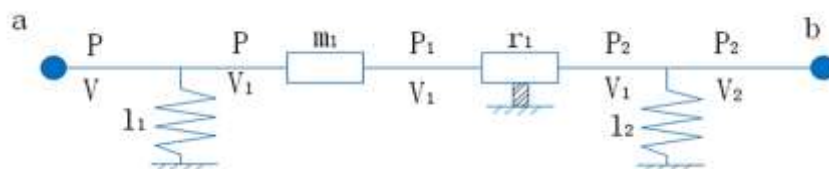


Figure 3. Hydraulic circuit.

The first is hydraulic, which takes into account elastic properties of a spring with pliability l_1 (pliability is the inverse of elasticity), inertial properties of a liquid by mass m_1 , pressure losses in the pipeline by means of active resistance r_1 . The third part is the centrifugal pump, and elastic properties of the spring with pliability l_1 (pliability is the value of the inverse elasticity) cylinder walls by active resistance. The first power circuit analyzes the hydraulic properties when the shock valve closes. This circuit comprises 2 components. The circuit link equations:

$$\begin{cases} P = m_1 \dot{V}_1 + r_1 V_1^2 + P_2 \\ V = l_1 \dot{P} + l_2 \dot{P}_2 + V_2 \end{cases} \quad (1)$$

Black box:



Figure 4. Black box for hydraulic energy circuit

Inside this system, it is imperative to compute not only the energy flow inside the hydraulic circuit, but also the energy transfer associated with heat. Figure 5 illustrates the section of the setup where heat transfer occurs.

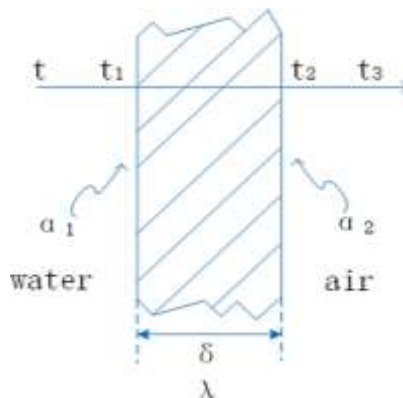


Figure 5. Part of the heat transfer plant. t - the temperature of hot water; t_1 , t_2 - wall temperature; t_3 - the temperature of the air; α_1 - convective heat transfer coefficient of water and left wall; α_2 - convective heat transfer coefficient of air and right wall; δ - the thickness of the wall surface; λ - Thermal conductivity of the wall

When the hot water flows, the convective heat transfer coefficient between the water and the left wall is h_1 , and the temperature of t is greater than t_1 , so the wall absorbs the heat brought by the hot water, and the wall temperature rises. When the temperature rises to t_1 , the surface temperature of the left wall is stable. The thickness of the wall is λ , and the heat is transmitted from the left wall to the right wall by means of heat conduction. When the temperature rises to t_2 , the surface temperature of the right wall reaches a stable state. The right wall carries out convective heat transfer with the air, and the convective heat transfer coefficient is h_2 . Through convective heat transfer, heat is transferred to the air until the air temperature t_3 reaches a stable state.

Calculate the convective heat transfer thermal resistance r_1 :

$$r_1 = \frac{1}{\alpha_1 F} \tag{2}$$

Calculate the convective heat transfer thermal resistance r_2 :

$$r_2 = \frac{\delta}{\lambda F} \tag{3}$$

Calculate the convective heat transfer thermal resistance r_3 :

$$r_3 = \frac{1}{\alpha_2 F} \tag{4}$$

Total thermal conductivity k :

$$k = \frac{1}{r_1 + r_2 + r_3} = \frac{1}{\frac{1}{\alpha_1 F} + \frac{\delta}{\lambda F} + \frac{1}{\alpha_2 F}} \tag{5}$$

Fig. 6. displays the energy flow within the heat transfer circuit.

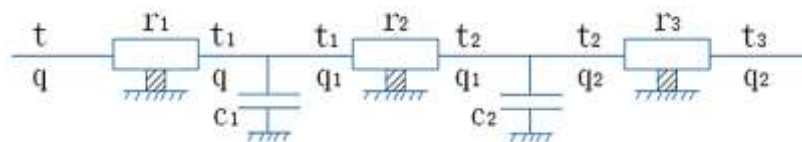


Figure 6. Heat transfer energy circuit

The circuit link equations:

$$\begin{cases} t = r_1 q + r_2 q_1 + r_3 q_2 + t_3 \\ q = c_1 \dot{t}_1 + c_2 \dot{t}_2 + q_2 \end{cases} \tag{6}$$

The input and output of the energy chain for thermal calculation are presented in the form of a “black” box. As shown in Figure 7.



Figure 7. Black box for heat transfer

The amplitude-frequency function of the energy loop is shown as follows:

$$A(j\Omega) = \sqrt{\text{Re}(j\Omega)^2 + \text{Im}(j\Omega)^2} \quad (7)$$

The phase frequency function of the energy loop is shown as follows:

$$\varphi(j\Omega) = -\text{arctg} \frac{\text{Im}(j\Omega)}{\text{Re}(j\Omega)} \quad (8)$$

About the frequency characteristic of constructing circuit, three parameters are changed to discuss.

The known conditions:

P - pressure, kPa; V - volume flow, l/s [liter per second]; r_1 - active resistances, $[kPa \cdot s^2 / lit]$; m_1 - mass of liquid, [kg]; l_1, l_2 - hydraulic compliance, $[lit \cdot s / Pa]$, 1 litre = 10^{-3} metre

Parameter are calculated or found from the experiment.

Are set by the input power of the circuit, for example $n_0 = 300$ W, as well as the inlet pressure $P_0 = 100$ kPa.

Hire the pressure loss on the active resistance is assumed $5 \pm 10\%$. The limit of change is accept, $\Omega = 1 \dots 10 \text{ rad} / s$. The circuit parameters are shown in Table 1.

Table 1

CIRCUIT PARAMETERS

m_1, kg	$r_1, [kPa \cdot s^2 / lit]$	$l_1, [lis \cdot s / Pa]$	$l_2, [lis \cdot s / Pa]$	P_{30}, kPa	$V_{30}, lit / s$
15	1.11	0.006	0.006	100	3
15	1.11	0.006	0.012	100	3
15	1.11	0.006	0.018	100	3

Dependency graphs are plotted based on the input values. For the best perception of graphs values are taken only those that affect the dependence. The values obtained for the first stage of the energy circuit are shown in Table 2.

Table 2

RECEIVED INFORMATION FOR HYDRAULIC

Ω	$Aj\Omega 1$	$\varphi j\Omega 1$	$Aj\Omega 2$	$\varphi j\Omega 2$	$Aj\Omega 3$	$\varphi j\Omega 3$
1	79.4657	-1.3146	53.8128	-0.8919	40.6789	-0.6541
2	65.4680	-4.3253	47.0320	-3.1108	36.6857	-2.3699
3	31.3059	-26.4915	26.7390	-22.4098	23.1995	-19.1536
4	133.9647	35.9101	228.3219	89.4271	135.1366	-36.4742
5	658.9842	-29.5785	135.9062	-5.8411	74.9429	-3.2893
6	297.2780	-4.8446	106.8818	-1.7378	65.1218	-1.1074
7	235.0341	-1.9376	97.5300	-0.8020	61.5242	-0.5433
8	210.7065	-1.0223	93.0622	-0.4498	59.7158	-0.3193
9	198.0383	-0.6207	90.5030	-0.2822	58.6519	-0.2090
10	190.4031	-0.4109	88.8736	-0.1905	57.9634	-0.1471

Based on the results of the calculation, the graphs of the amplitude frequency response and phase-frequency response and frequency response of the circuit are constructed. Further in these graphs are under construction:

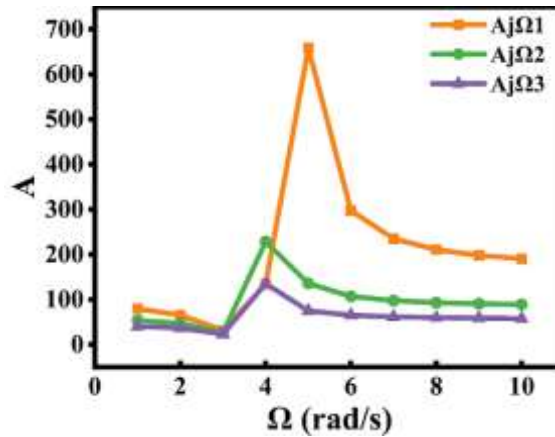


Figure 1. Amplitude frequency response

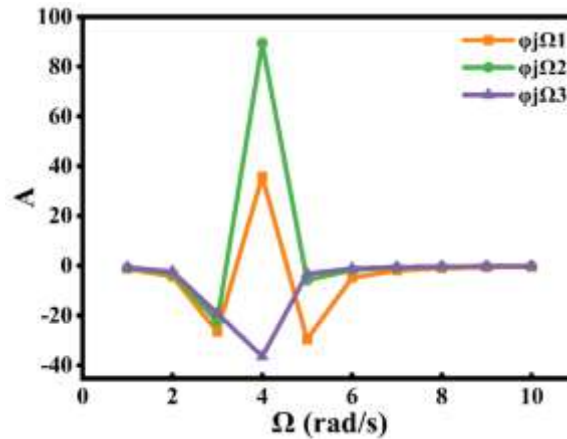


Figure 2. Phase frequency response

For power circuits of the heat transfer calculations are conducted similarly and are written in table 4. The thermal properties parameters used for calculations are shown in Table 3..

Table 3

PHYSICAL PROPERTY PARAMETER [10]

medium	temperature	μ	Pr	C_p	λ
Water (95°C-70°C)	90	0.3145	1.97	4.205	0.673
	80	0.3544	2.23	4.196	0.6669
	70	0.404	2.57	4.188	0.6595
Wall (68°C-60°C)	68	0.4165	2.656	4.187	0.65774
	65	0.43525	2.785	4.1855	0.6551
	60	0.4665	3	4.183	0.6507

Table 4

RECEIVED INFORMATION FOR HEAT TRANSFER

$r_1, [kPa \cdot s^2 / lit]$	$r_2, [kPa \cdot s^2 / lit]$	$r_3, [kPa \cdot s^2 / lit]$	$c_1, [l/s \cdot ^\circ C]$	$c_2, [l/s \cdot ^\circ C]$
0.000288	7.1429×10^{-6}	3.33×10^{-2}	0.001911	0.001911
0.000861	7.1429×10^{-6}	3.33×10^{-2}	0.002797	0.002797
0.001504	7.1429×10^{-6}	3.33×10^{-2}	0.004188	0.004188

The dependency graph is drawn based on input values. For optimal graph perception, take only those values that affect dependencies. The obtained values for the first stage of heat transfer are shown in Figure 10.

Table 2

VALUE AMPLITUDE FREQUENCY RESPONSE FOR ENERGY CIRCUIT

Ω	$A_{j\Omega 1}$	$\varphi_{j\Omega 1}$	$A_{j\Omega 2}$	$\varphi_{j\Omega 2}$	$A_{j\Omega 3}$	$\varphi_{j\Omega 3}$
1	0.0336	5.53737E-07	0.0342	7.00E-06	0.0348	3.13E-05
2	0.0336	1.10747E-06	0.0342	1.40E-05	0.0348	6.26E-05
3	0.0336	1.66121E-06	0.0342	2.10E-05	0.0348	9.39E-05
4	0.0336	2.21495E-06	0.0342	2.80E-05	0.0348	1.25E-04
5	0.0336	2.76869E-06	0.0342	3.50E-05	0.0348	1.57E-04
6	0.0336	3.32242E-06	0.0342	4.20E-05	0.0348	1.88E-04
7	0.0336	3.87616E-06	0.0342	4.90E-05	0.0348	2.19E-04
8	0.0336	4.4299E-06	0.0342	5.60E-05	0.0348	2.51E-04
9	0.0336	4.98363E-06	0.0342	6.30E-05	0.0348	2.82E-04
10	0.0336	5.53737E-06	0.0342	7.00E-05	0.0348	3.13E-04

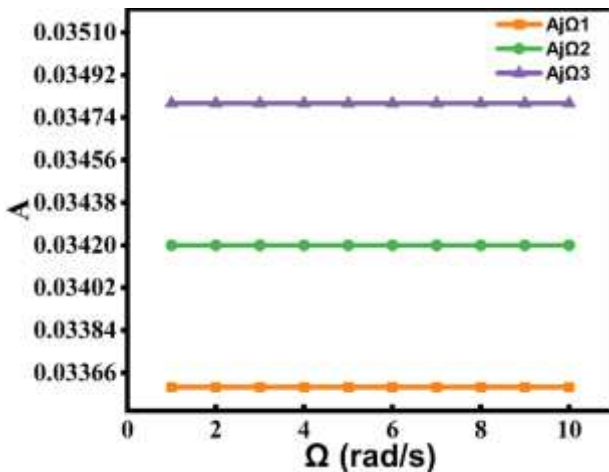


Figure 3. Amplitude frequency response

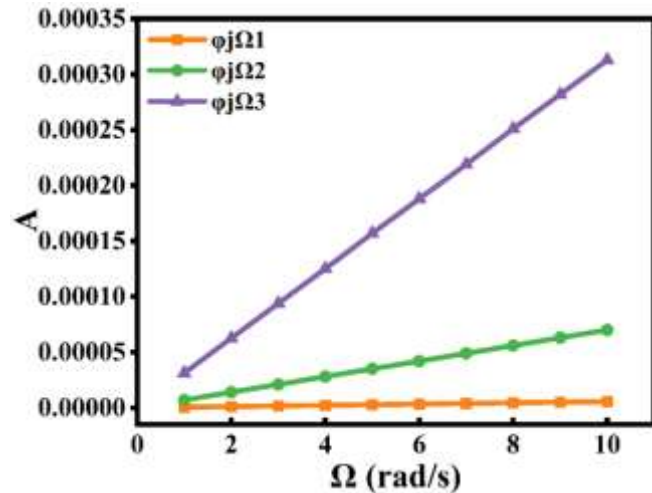


Figure 4. Phase frequency response.

The text discusses the issues related to the work and proposes potential solutions. A detailed description of the operational principle of the experimental device is presented together with a constructive scheme. The schematic diagram of the device's power circuit is created, with detailed explanations for each connection. Mathematical transformation of the power circuit yields complex impedance, frequency response function, amplitude-frequency characteristic, and phase-frequency characteristic. The circuit's frequency response is analyzed.

The experimental setup description is finished, and energy circuits for hydraulics and heat transfer are assembled.

Hydraulic energy circuits consider characteristics such as pressure, volume flow, hydraulic losses, hydraulic resistance, and hydraulic mass. Energy circuits for heat transfer consider characteristics such as mass flow rate, temperature, thermal resistance, and thermal power.

Displayed in Figure 1 and 2. When modeling the hydraulic power circuit, it was observed that as the frequency increases, the frequency response of the hydraulic circuit also increases and rapidly reaches its optimal value, causing the amplitude to drop. As the frequency rises, the pressure drop in the PFC of the hydraulic circuit decreases.

Figure 3 and 4 demonstrate that the frequency response of the hydraulic circuit diminishes as the frequency increases, resulting in consistent pulsations throughout the modeling of heat transfer in the energy circuit.

The generated graphs allow for tracing the relationship between two distinct attributes. The graph illustrates that for a specific r value, we reach the frequency peak more rapidly.

References:

1. Liu Y., Zhang J., Yu X., Qiu W., Liu Z. Mechanism and quantitative criterion of free vibration characteristics of hydraulic systems using the water hammer reflection coefficient // *Communications in Nonlinear Science and Numerical Simulation*. 2024. V. 133. P. 107959. <https://doi.org/10.1016/j.cnsns.2024.107959>
2. Wang C., Wang J., Guo Q., Ren X., Cao Y., Jiang D. Fixed-time adaptive neural control of electro-hydraulic system with model uncertainties: Theory and experiments // *Control Engineering Practice*. 2024. V. 147. P. 105931. <https://doi.org/10.1016/j.conengprac.2024.105931>
3. Lu Y., Tan L. Design method based on a new slip-diffusion parameter of centrifugal pump for multiple conditions in wide operation region // *Energy*. 2024. P. 130796. <https://doi.org/10.1016/j.energy.2024.130796>
4. Lv G., Yang X., Gao Y., Wang S., Xiao J., Zhang Y., Yang H. Investigation on fretting Wear performance of laser cladding WC/Co06 coating on 42CrMo steel for hydraulic damper // *International Journal of Refractory Metals and Hard Materials*. 2023. V. 111. P. 106068. <https://doi.org/10.1016/j.ijrmhm.2022.106068>
5. Li Y., Liu D., Cui B., Lin Z., Zheng Y., Ishnazarov O. Studying particle transport characteristics in centrifugal pumps under external vibration using CFD-DEM simulation // *Ocean Engineering*. 2024. V. 301. P. 117538. <https://doi.org/10.1016/j.oceaneng.2024.117538>
6. Wang B., Cheng F. R., Tang X. Z. Research on the complete vehicle control strategy of the composite accumulator hydraulic hybrid power system // *Journal of Energy Storage*. 2023. V. 74. P. 109384. <https://doi.org/10.1016/j.est.2023.109384>
7. Li S., Deng G., Hu Y., Yu M., Ma T. Optimization of structural parameters of pilot-operated control valve based on CFD and orthogonal method // *Results in Engineering*. 2024. P. 101914. <https://doi.org/10.1016/j.rineng.2024.101914>
8. Levitsev, A. P., Kudashev, S. F., Makeev, A. N., & Lysyakov, A. I. (2014). Vliyanie impul'snogo rezhima techeniya teplonosatelya na koeffitsient teploperedachi v plastinchatom teploobmennike sistemy goryachego vodosnabzheniya. *Sovremennye problemy nauki i obrazovaniya*, (2), 89-89. (in Russian).
9. Levitsev, A. P., Makeev, A. N., Makeev, N. F., Narvatov, Ya. A., & Golyanin, A. A. (2015). Obzor i analiz osnovnykh konstruktsii udarnykh klapanov dlya sozdaniya gidravlicheskogo udara. *Sovremennye problemy nauki i obrazovaniya*, (2-2), 188-188. (in Russian).
10. Aleksandrov, A. A., & Grigor'ev, B. A. (2006). *Tablitsy teplofizicheskikh svoystv vody i vodyanogo para*. Moscow. (in Russian).

Список литературы:

1. Liu, Y., Zhang, J., Yu, X., Qiu, W., & Liu, Z. (2024). Mechanism and quantitative criterion of free vibration characteristics of hydraulic systems using the water hammer reflection coefficient. *Communications in Nonlinear Science and Numerical Simulation*, 133, 107959. <https://doi.org/10.1016/j.cnsns.2024.107959>

2. Wang, C., Wang, J., Guo, Q., Ren, X., Cao, Y., & Jiang, D. (2024). Fixed-time adaptive neural control of electro-hydraulic system with model uncertainties: Theory and experiments. *Control Engineering Practice*, 147, 105931. <https://doi.org/10.1016/j.conengprac.2024.105931>
3. Lu, Y., & Tan, L. (2024). Design method based on a new slip-diffusion parameter of centrifugal pump for multiple conditions in wide operation region. *Energy*, 130796. <https://doi.org/10.1016/j.energy.2024.130796>
4. Lv, G., Yang, X., Gao, Y., Wang, S., Xiao, J., Zhang, Y., ... & Yang, H. (2023). Investigation on fretting Wear performance of laser cladding WC/Co06 coating on 42CrMo steel for hydraulic damper. *International Journal of Refractory Metals and Hard Materials*, 111, 106068. <https://doi.org/10.1016/j.ijrmhm.2022.106068>
5. Li, Y., Liu, D., Cui, B., Lin, Z., Zheng, Y., & Ishnazarov, O. (2024). Studying particle transport characteristics in centrifugal pumps under external vibration using CFD-DEM simulation. *Ocean Engineering*, 301, 117538. <https://doi.org/10.1016/j.oceaneng.2024.117538>
6. Wang, B., Cheng, F. R., & Tang, X. Z. (2023). Research on the complete vehicle control strategy of the composite accumulator hydraulic hybrid power system. *Journal of Energy Storage*, 74, 109384. <https://doi.org/10.1016/j.est.2023.109384>
7. Li, S., Deng, G., Hu, Y., Yu, M., & Ma, T. (2024). Optimization of structural parameters of pilot-operated control valve based on CFD and orthogonal method. *Results in Engineering*, 101914. <https://doi.org/10.1016/j.rineng.2024.101914>
8. Левцев А. П., Кудашев С. Ф., Макеев А. Н., Лысяков А. И. Влияние импульсного режима течения теплоносителя на коэффициент теплопередачи в пластинчатом теплообменнике системы горячего водоснабжения // Современные проблемы науки и образования. 2014. №2. С. 89-89.
9. Левцев А. П., Макеев А. Н., Макеев Н. Ф., Нарватов Я. А., Голянин А. А. Обзор и анализ основных конструкций ударных клапанов для создания гидравлического удара // Современные проблемы науки и образования. 2015. №2-2. С. 188-188.
10. Александров А. А., Григорьев Б. А. Таблицы теплофизических свойств воды и водяного пара. М.: МЭИ, 2006. 168 с. EDN RZDEKT.

Работа поступила
в редакцию 22.04.2024 г.

Принята к публикации
28.04.2024 г.

Ссылка для цитирования:

Fang Yilin, Kudashev S. Ways to Protect Equipment from Hydraulic Shock // Бюллетень науки и практики. 2024. Т. 10. №6. С. 296-305. <https://doi.org/10.33619/2414-2948/103/33>

Cite as (APA):

Fang, Yilin, & Kudashev, S. (2024). Ways to Protect Equipment from Hydraulic Shock. *Bulletin of Science and Practice*, 10(6), 296-305. <https://doi.org/10.33619/2414-2948/103/33>